

# A PARAMETRIC STUDY OF FAR-SIDE RESTRAINT MECHANICS

**Richard Kent, Jason Forman, David Lessley**

Center for Applied Biomechanics, University of Virginia  
USA

**Kristy Arbogast**

Children's Hospital of Philadelphia  
USA

**Kazuo Higuchi**

Takata

Japan

Paper Number 13-0381

## ABSTRACT

The goal of this study was to quantify the belt-torso interaction and whole-body kinematics in far-side lateral impacts and how they depend on shoulder-belt geometry, arm position, and belt pre-tensioning. A series of repeated 90-deg far-side impacts on three post-mortem human subjects was performed. A 3-d motion capture system measured skeletal kinematics. Arm position (Down, Slightly Up, Fully Up), D-ring location (Forward, Back, Intermediate), pre-tensioning (Yes, No), and impact severity (8g, 18g) were varied. Maximum lateral head excursion was found to be slightly sensitive to arm position and highly sensitive to D-ring location, pre-tensioning, and impact severity. An interaction between D-ring location and pre-tensioning was found, with the maximum pre-tensioning effect occurring at the Intermediate D-ring position. Limitations of this study include the use of repeated impacts and consideration of a single impact angle. 60-degree far-side oblique impacts are underway to assess the robustness of the conclusions drawn here.

## INTRODUCTION

A primary driver of contemporary seatbelt biomechanics research is the challenge of minimizing head excursion and the risk of a head contact with the vehicle interior, while simultaneously limiting belt impingement on the torso and concomitant belt-induced injuries. Many studies have evaluated this tradeoff in frontal impacts, but the topic has not been explored as much in other impact configurations. This tradeoff is particularly important in the far-side impact environment: head strikes are a key injury mechanism (e.g., Gabler et al. 2005) and belt characteristics such as pre-tensioning, D-ring position, and a second shoulder belt (e.g., Rouhana et al. 2006, Bostrom et al. 2008) can have a pronounced

influence on head excursion. Several far-side safety countermeasures have been proposed in recent years to address this injury mechanism, including in-board, seat-mounted airbags and deployment of far-side curtain airbags. The literature is lacking, however, a detailed description of the conditions influencing the ability of the standard 3-point seatbelt to restrain a human occupant in a far-side impact exposure. Horsch (1980) evaluated the dynamics of a belted anthropomorphic test device (ATD or crash test dummy) in collisions ranging from full frontal to full lateral, but no existing ATD is designed to replicate either the complex ipsilateral shoulder mechanics relevant to this situation or the oblique belt loading present on the contralateral lower torso. Efforts to create such an ATD are underway (e.g., the latest generation of the shoulder described by Törnvall 2008 is in evaluation testing now and the THOR dummy is nearing finalization), but post-mortem human subjects (PMHS) remain the most biofidelic model for studying these issues.

## METHODS

A series of repeated 90-deg far-side sled impacts was performed using three male post-mortem human subjects (Table 1). The subjects were acquired and prepared in accordance with the UVA Center for Applied Biomechanics Oversight Committee. The subjects were preserved by freezing and confirmed free of infectious diseases including HIV and Hepatitis B and C.

Subject kinematic data were measured using a 1000-Hz Vicon MX™ three-dimensional (3-d) camera-based motion capture system, which tracked the motion of retroreflective spherical markers through a calibrated 3D space within the cameras' collective field of view. The sled test fixture was designed to approximate a vehicle-based restraint environment while providing repeatable and reproducible test conditions and lines of sight for motion capture. The

design objectives of the test fixture included reducing test-to-test variability and increasing measurement capability through the use of simplified boundary conditions. For example, the subjects were positioned on a rigid planar seat with their torsos and heads supported by an adjustable set of plates to approximate a vehicle occupant's seated posture (i.e., the interaction with the seat was unlike that in an actual vehicle) (Figure 1).

**Table 1.**  
**Post-Mortem Test Subjects**

PMHS	Age	Stature	Weight	Cause of Death	Bone Quality*
551	67	173 cm	83 kg	Stroke	-0.6 (normal)
557	67	175 cm	91 kg	Pulmonary fibrosis	1.5 (above average)
559	60	170 cm	73 kg	Cardiac arrest (NFS)	-1.0 (borderline osteopenia)

\*DXA t-score, Total right femur

Restraint was provided by a 3-point shoulder and lap belt with lap-belt anchor positions approximating those in a typical mid-size sedan and a D-ring mount location representing the range present in the field. Four-marker clusters were secured to selected bones and rigid body mechanics was applied to determine the bone's 6-degree-of-freedom motion using a coordinate transformation. This test fixture and kinematic measurement method have been described in detail by Shaw et al. (2010) and Lessley et al. (2011).

Variations in arm position [Down (D), Slightly Up (SU), Fully Up (FU)], D-ring location [Forward (F), Back (B), Intermediate (I)] (Figure 2), pretensioning (PT) (Yes, No), and impact severity (8 g, 18 g) were studied. Every reasonable attempt was made to hold all other parameters constant across tests (e.g., initial position, impact conditions, restraint geometry). The arm position was based on the forward flexion angle of the humerus, with the Fully Up position representing the arms in a steering position. The two impact severities were chosen based on the field analysis reported by Gabler et al. (2005). The low-severity sled pulse, which had a total velocity change ( $\Delta V$ ) of 16 km/h, was based on the median severity of far-side tow-away crashes. The high-severity pulse, which had a  $\Delta V$  of 34 km/h, was based on the median severity of far-side field crashes in which MAIS 3+ injuries occurred (Figure 3). Repeated low-severity impacts were performed on each subject prior to a single, final high-severity impact. The ribs,

spine, and near-side shoulder were palpated for the presence of injury following each impact. The final test matrix included 15 sled tests (Table 2).

**Table 2.**  
**Sled Test Matrix**

Test	PMHS	Impact Severity	PT	Arm	D-ring
S0077	557	Low	N	SU	B
S0078	557	Low	N	D	B
S0079	557	Low	Y	D	B
S0080	557	Low	Y	SU	B
S0081	557	High	N	D	B
S0082	551	Low	Y	FU	F
S0083	551	Low	Y	D	F
S0084	551	Low	N	FU	F
S0085	551	Low	N	D	F
S0086	551	High	N	D	F
S0087	559	Low	N	D	F
S0088	559	Low	Y	D	F
S0089	559	Low	N	D	I
S0090	559	Low	Y	D	I
S0091	559	High	Y	D	I

Full-body computed tomography (CT) scans were taken of each subject prior to testing to confirm the absence of bony trauma. Dual-energy X-ray absorptiometry (DXA) assessed bone quality. After completion of the entire test battery, another full-body CT scan was taken and a detailed necropsy was performed to document the trauma sustained during the test series.

Instrumentation included tension gages on the shoulder belt near the D-ring and bilaterally near the lap belt mounts. The motion capture marker arrays were mounted to the skull, pelvis, first thoracic vertebra (T1), and both scapulae. Individual markers were adhered to the external surface of the subject from the mid-thoracic spine to the sacro-lumbar and at selected locations on the buck and along the belt webbing. Frontal, overhead, and oblique high-speed video cameras documented the tests at 1000 Hz.

The effects of the variations in test conditions were quantified by comparing sets of tests. For example, the effects of pre-tensioning were observed by comparing tests S0083 and S0085, and the interaction between D-ring position and pre-tensioning were observed by comparing tests S0087-S0090. Selected effects are reported in this paper, with a particular focus on belt loading, head excursion, and whole-body kinematics. The comparisons employ primarily the frontal video view, the tension gages, and reconstructions of the motion of bony structures using the motion capture data.

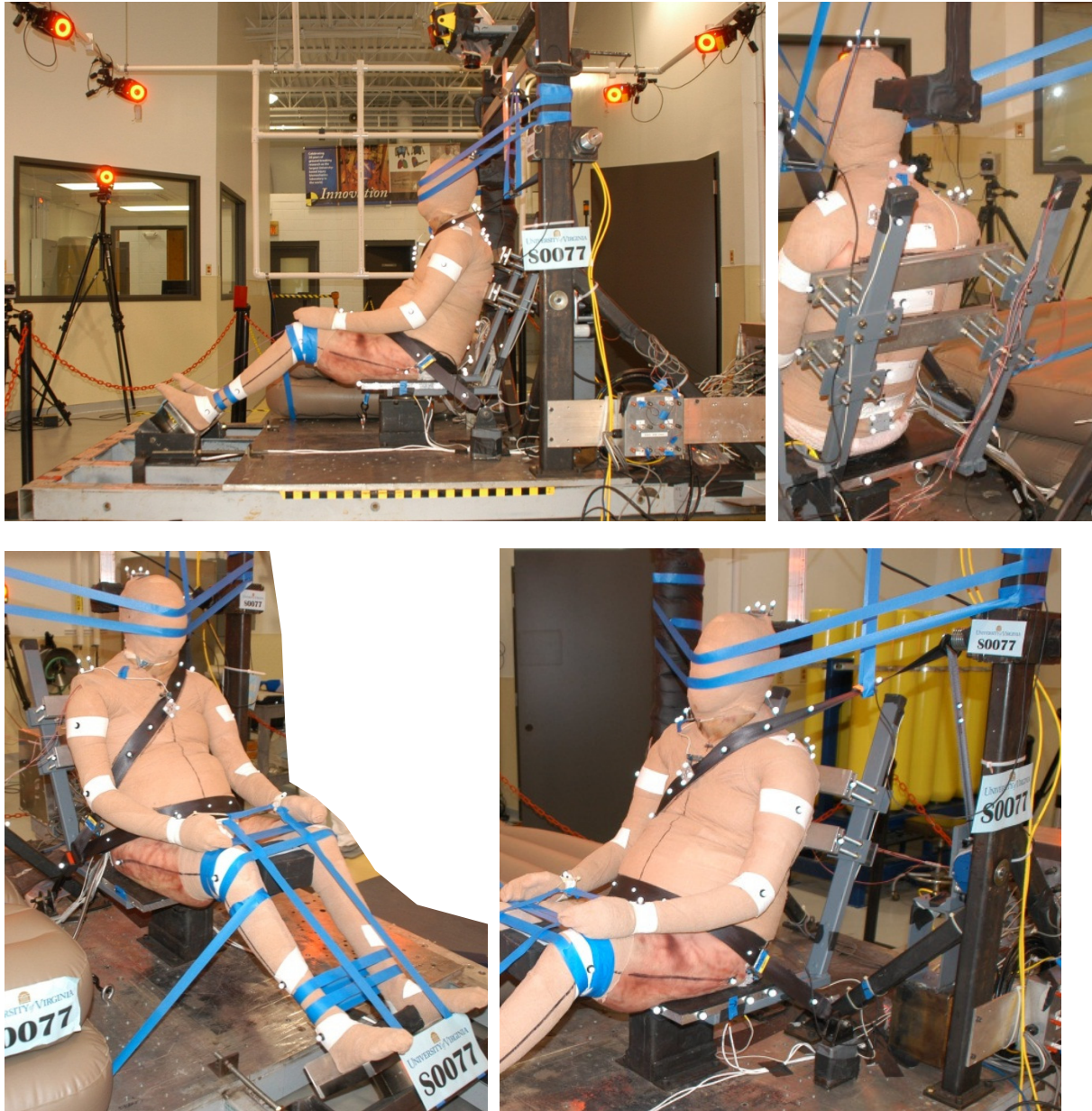


Figure 1. Photographs of the sled test fixture and an occupant positioned for testing. Masking tape used for positioning was partially severed immediately prior to test initiation. Sled motion simulated a far-side impact with the occupant moving right relative to the sled (away from the d-ring). These images depict the “Slight Up” arm position and the “Back” D-ring position.

The frontal video was mounted off-board, so the occupant’s motion relative to the buck is not necessarily reflected in the occupant’s position within the video frame. There was a vertical frame member on the buck that can be used as a qualitative reference point for excursion in these video views. The horizontal aluminum bars composing the seatback can also be used for this purpose as an occupant’s initial positioning on the sled was reproduced in all tests. In the

reconstructions of the bony motion, computed tomography (CT) images of the test subjects were used to illustrate the rigid body motion of the head, shoulder girdle, sternum, and pelvis relative to the buck.

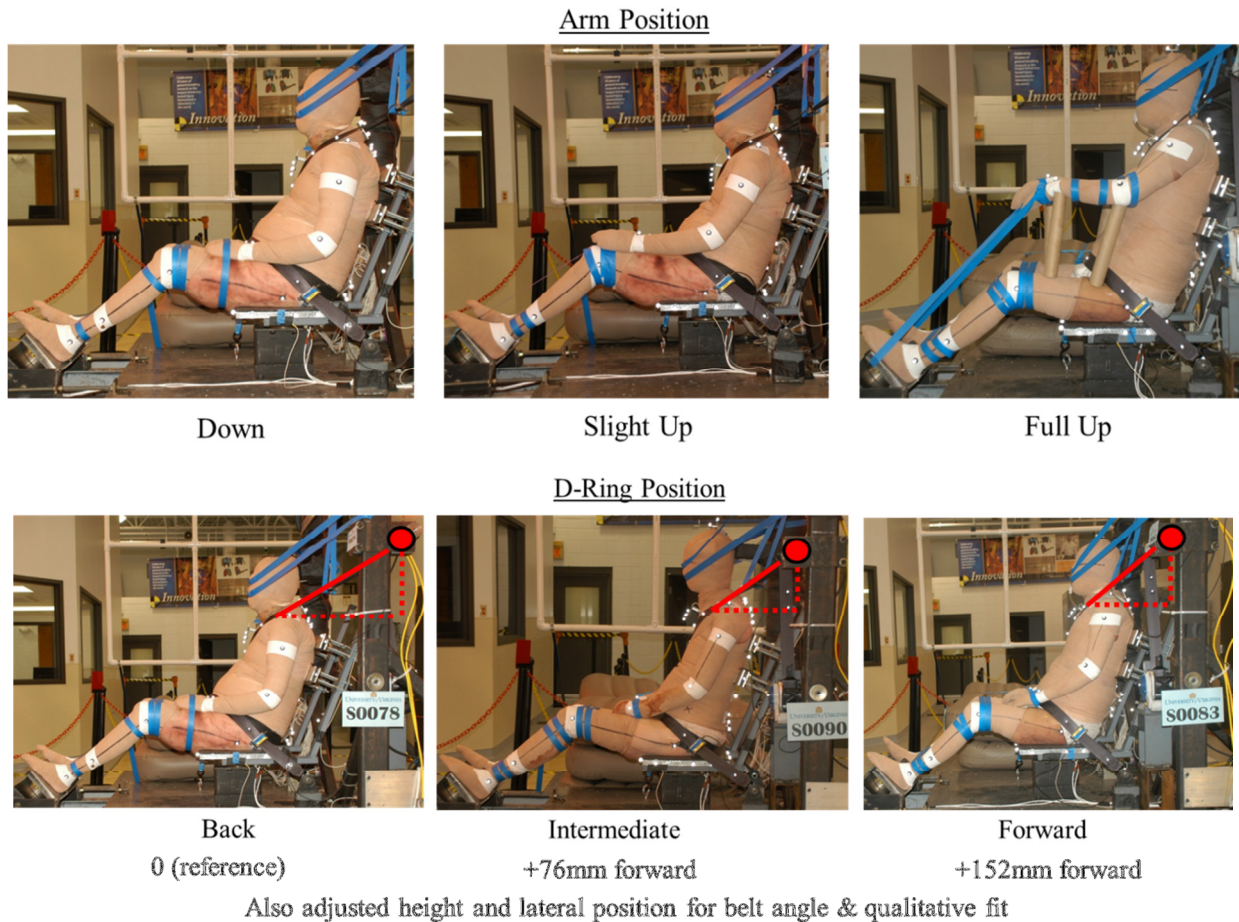


Figure 2. Photographs depicting variation in arm and D-ring position.

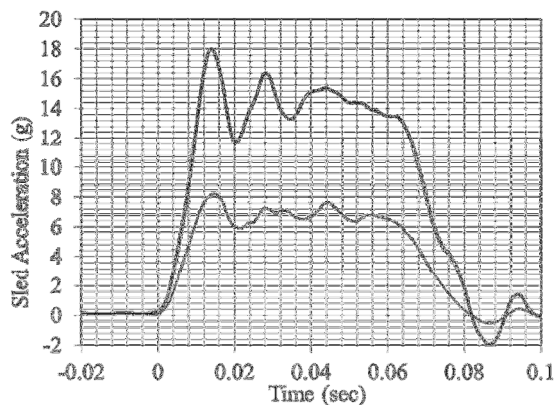


Figure 3. Lateral sled acceleration in low-severity and high-severity tests.

## RESULTS

### Arm Position

Arm position had the least influence of the parameters studied. Comparison of tests S0084

and S0085, for example, revealed a decrease of only 5.8 mm in the peak lateral excursion of the left acromio-clavicular (AC) joint when the arm was Fully Up, which translated into a decrease of only 6.1 mm in peak lateral head excursion. In contrast, pre-tensioning and the fore-aft location of the D-ring substantially affected occupant kinematics, as described in detail below.

### Influence of Pre-tensioning

Comparison of S0077 with S0080 shows the influence of pre-tensioning with the D-ring in the back position. The frontal video view illustrates the decreased shoulder motion with the pre-tensioned system and the resulting reduction in lateral head excursion relative to the buck (Figure 4). Reconstruction of the bony motion shows the pronounced reduction in lateral motion of the head, shoulder girdle, and pelvis relative to the buck (Figure 5). The peak values of lateral excursion relative to the buck of the centers-of-gravity of the head, T1, sternum and pelvis, and of the acromio-

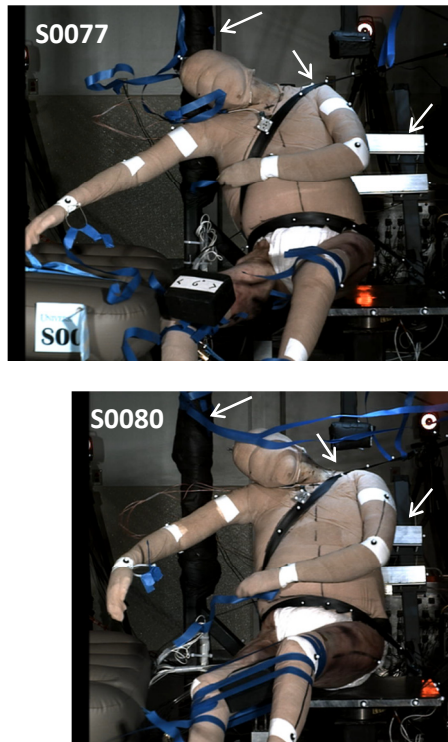


Figure 4. Frontal video views illustrating shoulder retention and head excursion without (S0077, top) and with (S0080, bottom) a pre-tensioner. Arrows point to a vertical rail on the sled and the aluminum bars on the seatback (which provide reference for the excursion) and the shoulder movement relative to the webbing.

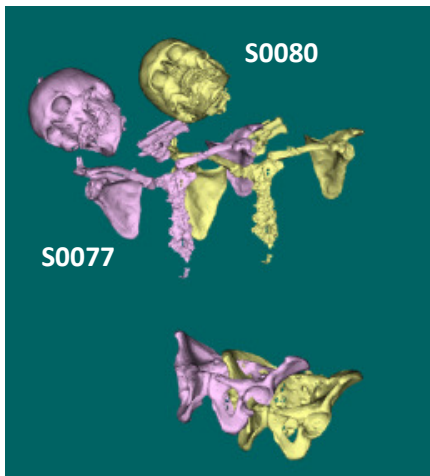


Figure 5. Anterior view of CT reconstructions of the head, shoulder, sternum, and pelvic positions and orientations at the time of peak head excursion relative to the buck. Yellow images are subject 557 in test S0080 (with PT). Purple images are the same subject in test S0077 (no PT).

clavicular joints, are reported in Table 3. The peak lateral excursion of the head was 151.2 mm less in test S0080 than in test S0077, of T1 was 150.1 mm less, of the left AC joint was 147.7 mm less, of the right AC joint was 148.9 mm less, and of the pelvis was 60.4 mm less (Table 3).

The influence of pre-tensioning is apparent in the shoulder-belt tension. Even though the tests were purely lateral, over 2 kN of tension was generated in the shoulder belt and the pre-tensioner reduced the system response time by approximately 40 ms (Figure 6). The peak belt tension was similar with and without pre-tensioning.

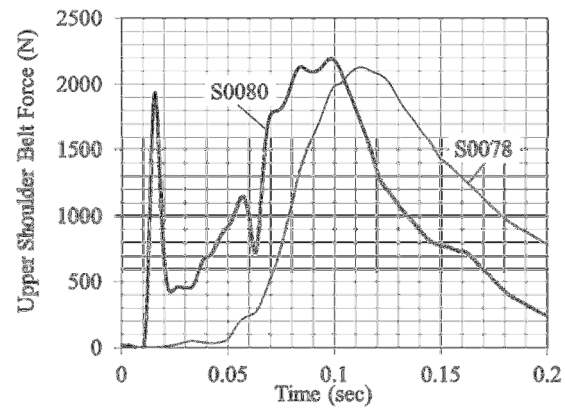


Figure 6. Tension in the shoulder belt in test S0080 (with PT) and test S0077 (no PT).

### Influence of D-ring Position

Restraint mechanics were less sensitive to D-ring position than they were to pre-tensioning (Figure 7). Comparison of S0087 with S0089 shows the influence of moving the D-ring 76 mm anteriorly in the absence of pre-tensioning. The peak lateral excursion of the head was 57.4 mm less in test S0089 (Intermediate D-ring position) than in test S0087 (Forward D-ring position), of T1 was 53.0 mm less, of the left AC joint was 67.0 mm less, of the right AC joint was 27.3 mm less, and of the pelvis was 28.2 mm less (Table 3). Comparison of S0088 with S0090 shows the influence of moving the D-ring 76 mm anteriorly with pre-tensioning. The peak lateral excursion of the head was 43.3 mm less in test S0090 (Intermediate D-ring position) than in test S0088 (Forward D-ring position), of T1 was 13.5 mm less, of the left AC joint was 14.4 mm less, of the right AC joint was 10.5 mm less, and of the pelvis was 53.2 mm less (Table 3).

**Table 3.**  
**Peak Lateral Excursion\***

Test	Head	T1	Pelvis	AC joint (L)	AC joint (R)
S0077	454.4 195	317.4 145	193.0 139	316.7 173	312.1 145
S0078	418.5 179	279.8 140	181.6 138	287.5 146	273.3 138
S0079	302.9 152	179.3 115	152.0 100	180.6 115	175.8 115
S0080	303.2 147	167.3 115	132.6 104	169.0 121	163.2 110
S0081	571.2 126	413.0 110	313.2 115	437.6 120	412.1 115
S0082	251.5 126	160.2 111	146.5 110	146.6 111	160.5 108
S0083	235.8 127	136.5 111	145.8 111	138.5 111	135.9 96
S0084	379.3 173	265.2 140	186.2 133	258.2 169	266.7 131
S0085	373.2 174	240.2 129	160.9 114	264.0 179	238.1 128
S0086	632.8 147	466.8 138	287.1 100	528.6 150	432.1 118
S0087	503.2 268	346.4 284	174.4 132	391.5 284	317.8 284
S0088	264.7 158	143.7 113	120.1 107	141.2 190	144.5 110
S0089	445.9 222	293.4 271	202.6 143	324.5 271	290.5 142
S0090	221.4 143	130.2 112	173.3 115	126.8 101	134.0 104
S0091	494.8 130	325.4 115	287.9 106	342.4 133	336.4 113

\*Top number is the peak lateral excursion in mm. Bottom number is the time of peak lateral excursion in ms.

### Pre-tensioning and D-ring position

Peak excursion was more influenced by pre-tensioning than by D-ring position, but there were interactions between the two parameters. As shown in Figure 8, the reduction in head excursion associated with pre-tensioning was substantial regardless of D-ring position, but it was more pronounced in the Intermediate D-ring position (50.3%) than in either the Forward (39.3%) or Back (30.5%) positions.

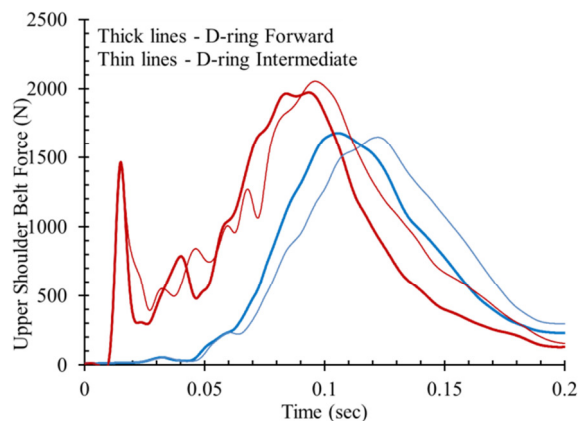


Figure 7. Tension in the shoulder belt in tests S0087 through S0090 illustrating the role of pre-tensioning (red vs. blue lines) and D-ring position (thick vs. thin lines).

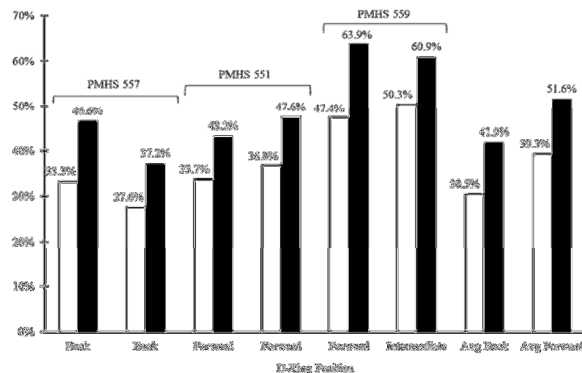


Figure 8. Reduction in peak lateral excursion when a pre-tensioner was used (low-severity tests). White bars are the head. Black bars are the left AC joint.

Comparison of peaks does not fully elucidate these interactions, however, as there is a pronounced difference in the timing of those peaks. It is informative to compare whole-body positions at concurrent time points, as shown in Figure 9. The test with the pre-tensioned belt mounted at the Intermediate D-ring position generated substantially more restraint through the left shoulder as compared to the other test conditions. This resulted in less right-lateral rotation of the torso in addition to the overall reduction in peak head excursion. Furthermore, this peak excursion was attained earlier (143 ms in S0090 vs. 158 ms in S0088, 222 ms in S0089, and 268 ms in S0087).

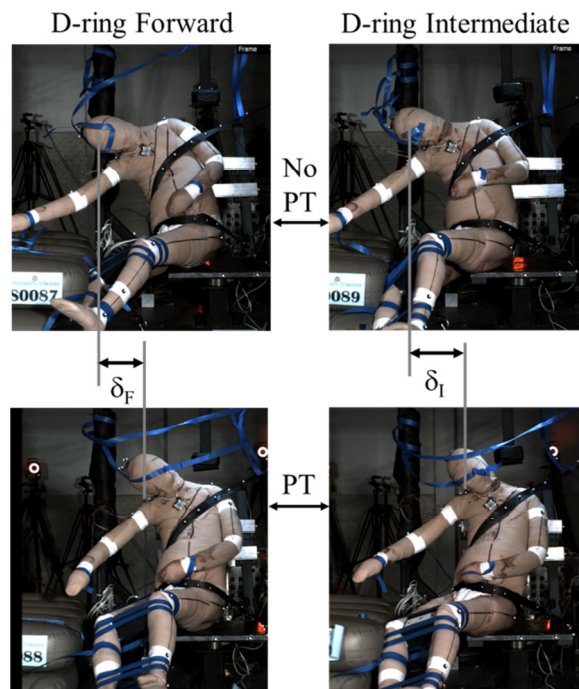


Figure 9. Video frames from tests S0087 through S0090 at peak head excursion illustrating the interaction between D-ring position and pre-tensioning. Note that the effect of pre-tensioning is more pronounced with the Intermediate D-ring position than with the Forward position ( $\delta_I > \delta_F$ ).

### High-Severity Impacts and Injury Outcome

The PMHS exhibited distinct patterns of trauma. Subject 559, whose high-severity test involved a pre-tensioned belt with the Intermediate D-ring position, sustained a sternal fracture and 24 fractures on 14 ribs, including a left posterior fracture on rib 11. There was a concentration of fractures in the right lower aspect in the region of heavy shoulder belt loading. Blood was also found in this subject's peritoneal cavity, though no acute laceration was identified. Finally, a fracture of the anterior vertebral body of T9/10 was found in this subject.

Subject 551, whose high-severity test involved no pre-tensioner and the Forward D-ring position, sustained 3 rib fractures, all on the left side and two of which were posterior on ribs 11 and 12. This subject also sustained AIS 2 soft tissue injuries with a facet dislocation on the left aspect of the cervical spine at the level of C6/7. The anterior longitudinal ligament was completely ruptured and soft tissue disruption was identified in the posterior longitudinal ligament, the facet joint capsule, the ligamentum flavum, the interspinous ligament, and the intervertebral disc, which was separated from the

vertebra on the left side. Note that all of this trauma was on the left aspect, which was the side put into tension by the restraining forces pulling left on the torso and pelvis and the head's inertia placing the cervical spine into right lateral bending.

Subject 557, whose high-severity impact involved no pre-tensioning and the Back D-ring position, sustained 26 rib fractures, including 4 posterior fractures on the left ribs 7-10. Again, these fractures were concentrated in the lower right quadrant.

### DISCUSSION

This study is the first report of PMHS tested in a parametric manner exploring the influence of arm position, D-ring position, and pre-tensioning on restraint mechanics in a far-side 90° exposure. In addition to quantifying the motion of several bony structures, this study reports three key findings.

First, as illustrated in the upper-left image of Figure 9, a 3-point harness applies substantial restraining force to an occupant in a far-side impact, even when the D-ring is in a forward position and there is no pre-tensioning. This restraining force and the resulting kinematics are influenced weakly by the position of the humerus and more strongly by the anterior-posterior position of the D-ring and by the presence of pre-tensioning.

Second, there is an interaction between the position of the D-ring and the effectiveness of the pre-tensioner. In these tests, the Back D-ring position facilitated the development of relatively large restraining force within the shoulder belt regardless of the presence of a pre-tensioner, which reduced the role of pre-tensioning relative to the Intermediate D-ring position. Conversely, with the Forward D-ring position, the shoulder belt was less able to engage the shoulder regardless of the presence of a pre-tensioner. With the Forward D-ring position, the pre-tensioning did not engage the shoulder since the belt angle was such that during pre-tensioning the webbing just translated along a path essentially tangent to the clavicle. In order for belt webbing to generate force normal to its path, it must undergo a change in angle. If the D-ring is positioned such that the webbing changes angle as it passes over the shoulder, then pre-tensioning will apply restraining force to the shoulder. If the D-ring is too far forward for that angle change to occur, then the role of pre-tensioning is limited to pre-loading the lower, contralateral aspect of the torso and the effectiveness of the pre-tensioner as a mitigator of head excursion, while still present, is reduced.

Finally, this study identified a tradeoff between thoracic engagement, head excursion, and injury to the cervical spine. A comparison of the magnitude of injury generated in these PMHS is confounded by the differences in bone quality across subjects, but some general observations can be made. When torso engagement is maximized, there is an increased risk of thoracic injury but a decrease in head excursion. The rib cage is more easily injured by lower, oblique loading than by frontal loading to the superior ribs or loading to the shoulder. While shoulder engagement is an important aspect of restraint in these impacts, a substantial portion of restraining force passes through the lower portion of the contralateral rib cage (Figure 10). Future research should include detailed studies of how the geometry and force-generating characteristics (pre-tensioners, load-limiters, etc.) of a belt system influence the apportionment of loading through the ipsilateral shoulder (a strong anatomical load path) and the contralateral torso (less strong), and how that apportionment influences head trajectory. Furthermore, this study showed that effective restraint engagement of the torso can

generate lateral bending of the cervical spine sufficient to generate injury from head inertia. These tradeoffs reflect the complex interactions among belt geometry and structural mechanics, whole-body kinematics, and injury mechanisms in far-side crash loading. These interactions are at least as complex as they are in frontal crashes, and significant research will be required to understand them fully. For example, the left posterior rib fractures generated in these tests are unlike the fracture patterns generated in frontal sled tests of restrained cadavers and their mechanism, while unknown, is probably related to the complex rib cage deformations generated by the belt heavily loading the lower-right torso.

The key limitation of this study for application to the in-vehicle environment is the use of simplified boundary conditions. The load paths generated by interaction with the seat pan, seat back, and center console in a vehicle are either understated or ignored completely in this test configuration. The findings should be evaluated in that light.

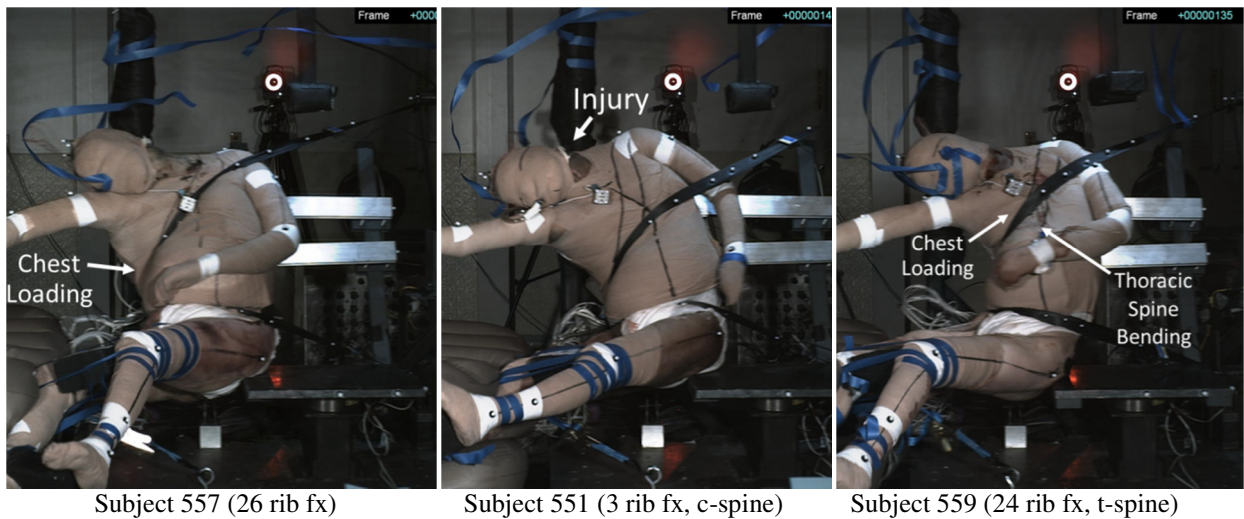


Figure 10. Video frames from tests S0081, S0086, and S0091 (the high-severity tests) at peak head excursion illustrating the interaction between restraint mechanics, whole-body kinematics, and injury mechanisms. Note that the increased torso engagement on subjects 557 (Back D-ring position) and 559 (Pre-tensioned belt) reduced head excursion relative to subject 551 (Forward D-ring, no Pre-tensioner), but was also associated with increased trauma to the torso. Subject 551 sustained less torso trauma, but the reduced torso engagement allowed greater head excursion and the subject sustained cervical spine trauma on the tension side of the neck during lateral bending as the neck arrested the lateral motion of the head.

## CONCLUSIONS

This study documented whole-body kinematics and restraint mechanics in a far-side collision. Detailed skeletal measurements and a parametric study design allowed for a detailed assessment of the roles of fore/aft D-ring position, arm position,

pre-tensioning, and impact speed. An interaction between D-ring position and pre-tensioning was identified, with the effect of pre-tensioning being greatest at the Intermediate D-ring position. Injury tradeoffs were also identified.

## REFERENCES

Bostrom, O., Gabler, H., Digges, K., Fildes, B., Sunnevang, C. (2008) Injury reduction opportunities of far side impact countermeasures. *Ann Adv Automot Med* 52:289-300.

Gabler, H. C., Fitzharris, M., Scully, J., Fildes, B. N., Digges, K., Sparke, L., (2005). Far side impact injury risk for belted occupants in Australia and the United States. Proceedings of the International Technical Conference on the Enhanced Safety of Vehicles, Paper No.05-0420.

Horsch, J. (1980) Occupant dynamics as a function of impact angle and belt restraint. Paper 801310, Society of Automotive Engineers, Warrendale, PA.

Lessley, D., Shaw, G., Riley, P., Forman, J., Crandall, J. (2011) Assessment and validation of a methodology for measuring anatomical kinematics of restrained occupants during motor vehicle collisions. *J Biosens Bioelectron* S1:002. doi: 10.4172/2155-6210.S1-002.

Rouhana, S., et al. (2006) Biomechanics of 4-point seat belt systems in farside impacts. *Stapp Car Crash J*. Vol. 50.

Shaw, G. et al. (2009) Impact response of restrained PMHS in frontal sled tests: Skeletal deformation patterns under seat belt loading. *Stapp Car Crash J* 53:1-48.

Törnvall, F. (2008) Development of a new shoulder for the THOR dummy intended for oblique collisions. Doctoral thesis, Chalmers University, Göteborg, Sweden.